SCIENCE CHINA
Technological Sciences

•Article•

July 2022 Vol.65 No.7: 1513–1523
https://doi.org/10.1007/s11431-021-2028-6

Control of myoelectric prosthetic hand with a novel proximity-tactile sensor

YANG Bin[1], JIANG Li[1*], GE ChuanYang[1,2], CHENG Ming[1] & ZHANG Jia[1,2]

[1] State Key Laboratory of Robotics and System, Harbin Institute of Technology, Harbin 150080, China;
[2] Key Laboratory of Microsystems and Microstructure Manufacturing Ministry of Education, Harbin Institute of Technology, Harbin 150080, China

Received December 26, 2021; accepted March 7, 2022; published online June 2, 2022

Currently, prosthetic hands can only achieve several prespecified and discrete hand motion patterns from popular myoelectric control schemes using electromyography (EMG) signals. To achieve continuous and stable grasping within the discrete motion pattern, this paper proposes a control strategy using a customized, flexible capacitance-based proximity-tactile sensor. This sensor is integrated at the fingertip and measures the distance and force before and after contact with an object. During the pre-grasping phase, each fingertip's position is controlled based on the distance between the fingertip and the object to make all fingertips synchronously approach the object at the same distance. Once contact is established, the sensor turns to output the tactile information, by which the contact force of each fingertip is finely controlled. Finally, the method is introduced into the human-machine interaction control for a myoelectric prosthetic hand. The experimental results demonstrate that continuous and stable grasping could be achieved by the proposed control method within the subject's discrete EMG motion mode. The subject also obtained tactile feedback through the transcutaneous electrical nerve stimulation after contact.

prosthetic hand, proximity, tactile sensor, myoelectric control, sensory feedback

Citation: Yang B, Jiang L, Ge C Y, et al. Control of myoelectric prosthetic hand with a novel proximity-tactile sensor. Sci China Tech Sci, 2022, 65: 1513–1523, https://doi.org/10.1007/s11431-021-2028-6

1 Introduction

The mechanical structure of prosthetic hands for upper-limb amputees has reached a very high level, especially dexterous multi-fingered prosthetic hands with multiple active degrees of freedoms (DoFs) [1]. Their mechatronics system enables many possible grasping patterns. However, due to the limitation of the sensing ability and human-machine neural interface, the hardware potential of the prosthesis cannot be fully realized as there are insufficient control inputs for the activation of all possible grasping patterns. Moreover, since the spatial properties of the grasped object cannot be sensed, the prosthetic hand cannot easily control the fingers finely to adapt to an object in the discrete and finger-coupled motion patterns before grasping, resulting in the impaired continuity and stability of grasping.

Accordingly, many studies have proposed various non-invasive methods for controlling prosthetic hands, such as electroencephalography-based brain-computer interface [2] and flex sensors attached to fingers [3]. These methods can allow the prosthetic or extra robotic hand to trigger opening and closing while not enabling many possible closing patterns of the multiple active DoF hand or are not suitable for transradial amputees. For the sake of non-invasiveness and simplicity, surface electromyography (EMG) control of the stumps of amputees is the most popular method to control

*Corresponding author (email: jiangli01@hit.edu.cn)

prosthetic hands [4]. For multi-fingered myoelectric prosthetic hands, the mainstream control methods include sequential control and coding control based on switching strategies [5,6], pattern recognition-based motion classification [7], and simultaneous proportional control [8]. Pattern recognition control strategies use multiple EMG electrodes to identify muscle contraction, recognizing up to 19 hand movements [9]. The method based on the switching strategy uses EMG signals as the switching signals to switch between pre-set motion patterns. However, these methods only output a number of prespecified and discrete hand motion patterns. In addition, simultaneous proportional control can only achieve simultaneous continuous control with limited DoFs (2–3) now, and the motion decoding precision and accuracy are limited [10]. Thus, the control methods of outputting various discrete hand motion patterns are currently the most popular. Limited control outputs cannot fully use all possible gestures of the multi-fingered hand. In each discrete hand motion pattern, all fingers move along their pre-set trajectory and cannot form the optimal grasp configuration according to the object shape. Moreover, the shape, position, and pose of the grasped object are uncertain in daily life. Thus, when only using EMG control, all fingers may not simultaneously touch the object. Some fingers make premature contact, which may let the object move out of the hand's reach or topple the object. Thus, the user needs to monitor the grasping process all the time and move the arm to adjust the position and posture of the entire prosthetic hand to grasp the object as stably as possible. This control method increases the user's physical strength and attention consumption and reduces the continuity of grasping. Thus, the prosthetic hand should preadjust each finger to form a suitable grasping gesture and adapt to the grasped object [11].

This problem can be solved in two ways based on monitoring force and planning grasp. Some studies employed tactile or motor current sensors to detect contact and control each finger [12,13]. However, this solution is based on physical contact. That is, sensors have to actually touch to obtain useful information, which may still cause a light object significant motion. Moreover, the underactuated prosthetic hand could automatically adapt to the shape of the object after contact [14], but this could also knock the object over or move it out of the grasp. The touch-and-slippage detection algorithm based on the normal contact force could make the prosthetic hand effectively grasp the object [15]. This compensation response action can only be performed after the beginning of the slippage events, and the contact state of the force sensor also limits the success rate. Therefore, non-contact sensing methods, usually vision or optical based, are used to obtain an object's spatial information [16,17]. However, vision suffers from occlusion, size, and real-time constraints. Optical-based sensors are highly sensitive to the reflectivity of objects. Moreover, rigid components are difficult to be attached to the curved surface of prosthetic hands.

Thus, the simple capacitance-based proximity sensor is used [18,19]. Non-contact proximity sensors can be used to measure the distance of objects and control the robot, such as maintaining a safe distance and avoiding collisions in unknown or partially modeled environments [20]. The robot can perform feedforward control based on proximity sensing to improve the grasp performance prior to contact [21,22]. Some researchers have used proximity sensors on a two-fingers parallel gripper to control the finger velocity according to the object's distance and to securely grasp the easily deformable object [23]. A prosthetic hand with rigid proximity sensors estimated the object's shape according to the distance between each finger and the surface and then selected a grasping pattern [24]. However, the finger could not be controlled finely.

In addition, tactile sensing is widely considered an essential capability for efficient grasping and manipulation [25]. The sensorimotor system is the basis of human grasping, and an able-bodied person often performs tactile servo actions almost subconsciously [26], but transradial amputees lost this capacity. Commercial prostheses suffer a lack of tactile sensing. Although some advanced prosthetic hands are equipped with tactile sensors, tactile information is only used for prostheses automatic control and cannot be transmitted to users. Users cannot accurately control grasping without perception of the actual grasping force [27]. Moreover, the absence of sensory feedback results in foreign body sensation and reduces the acceptance rate of the prosthetic hand [28].

To restore the amputee's tactile perception ability, external physical stimuli controlled by the grasping force stimulate the skin to produce sensations [29]. Compared with the open-loop control without sensory feedback, the one with sensory feedback significantly improves the grasping ability [30].

To obtain proximity and tactile sensing, multiple discrete single-sensing sensors are required [31], which will bring complexity to the space layout and acquisition circuit. Moreover, most sensors are rigid and large, not suitable for prostheses' compact structure and irregular contact surfaces [32]. Some studies have developed multimodal sensors to reduce the hardware burden, which has proximity and tactile sensing [33,34]. But the sizes of the sensors are large, it is difficult to accurately measure the contact force.

In response to the problem, in this study, a customized, flexible proximity-tactile sensor (PTS) was employed to improve the grasping performance of the prosthetic hand. We designed an integrated sensor measurement system. We used the sensor to realize pre-grasping gestures based on proximity sensing and fingertip force control based on tactile sensing. Furthermore, we performed the man-machine closed-loop prosthetic hand control based on proximity and tactile sensing through the neural interface.

2 Materials and methods

This work used the fifth-generation prosthetic hand developed by the Harbin Institute of Technology (HIT V hand) [35]. Figure 1(a) shows the prototype system of the prosthesis with the customized PTSs. The HIT V hand has five modular fingers. Each finger has two flexion joints coupled by a tendon and is actuated by a DC motor mounted inside the finger. A commercial joint angle sensor measures the joint angle. In addition, each fingertip is equipped with a flexible PTS to sense the proximity and contact force. For the expansion of the electrical system, all motors and sensors are controlled by an external customized prosthetic hand controller. The myoelectric control of the HIT V hand has been demonstrated in ref. [6].

2.1 Prototype flexible PTS

Figure 1(b) and (c) shows the structure and working principle of the proposed flexible PTS. A parallel plate capacitor comprises two parallel electrode plates and a dielectric between them. Ideally, the charge on each plate will be spread evenly on the inside surface of each plate, and the uniform electric field between the plates of a capacitor will be constant and directed perpendicularly to the electrode surface. Conversely, in reality, due to the effect of the finite plate width, there is a fringing field around the periphery of the plates outside the capacitor, as shown in Figure 1(c). When the object is close to the plate, an electric field exists between the object and the top plate, which leads to the change in the capacitance value between the two parallel plates. As shown

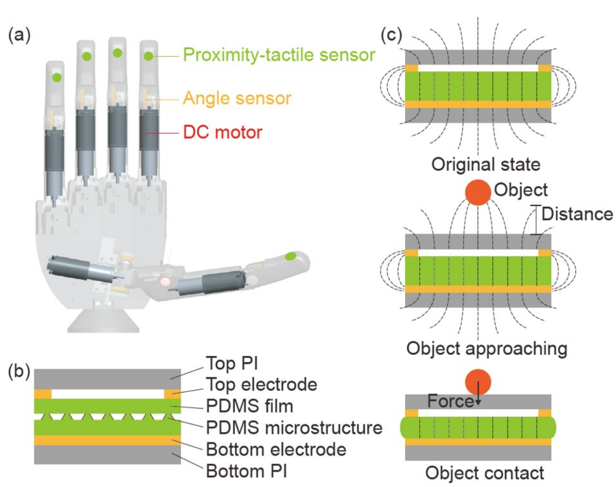

Figure 1 (Color online) (a) Schematic of the HIT V prosthetic hand equipped with proximity-tactile and angle sensors. The hand has six DC motors for each finger and the thumb ab/ad. (b) Structure of the proximity-tactile sensor. (c) Working principle of the proximity-tactile sensor.

in Figure 1(c), the capacitance value between the parallel plates reduces as the distance between the object and the plate decreases. In this work, the top plate electrode of the PTS is ring-shaped, and the bottom plate is still a round electrode. Compared with the round electrode, the side area of the ring-shaped electrode is increased so that more charges are concentrated on the side of the electrode. This design enhances the fringing field of the capacitor. Simultaneously, it reduces the effective areas of the top and bottom plates; the electric field between the two plates reduces. Thus, the strength of the fringing field increases relatively, which eventually strengthens the proximity sensing ability of the PTS. After the object touches the top plate, as shown in Figure 1(c), the dielectric layer deforms under contact force, and the distance between the top and bottom plates reduces. According to the parallel plate capacitance calculation, the capacitance value between two plates increases. To improve the tactile sensitivity, a pyramidal microstructure and the air gap are introduced in the dielectric layer to reduce the elastic modulus, which enhances the tactile sensitivity and shortens the response time. The effective cell diameter of the PTS is 3 mm, and the total thickness is 900 μm. In addition, the entire sensor is encapsulated using a flexible silicone. The sensor can be attached to the fingertips of the HIT V hand.

2.2 Integrated design of the PTS system

The proposed flexible-tactile sensor is based on capacitance measurement. It is attached to the fingertip surface, very close to the motor mounted inside the proximal phalanx of the finger. Therefore, the electromagnetic noise of the motor should be considered. In addition, the output capacitance of the sensor is in the order of sub-pF within the measuring range, so the sensor is susceptible to external interference, such as the parasitic capacitance of the system and mechanical vibration of the connecting wires. Hence, the measurement circuit should be close to the sensor.

We designed a compact measurement system. The measurement circuit board was installed inside the fingertip cavity, and the sensor's electrodes were connected to the circuit board through enameled wires. They were fixed on the distal phalanx of the finger, and there was no relative movement when the finger moved. The connection wires between the measuring circuit and outside were only the digital signal and power line, which ensured the accuracy and reliability of the measurement. A capacitance measurement ASIC (FDC2214, Texas Instruments, Texas, USA) was used to measure the capacitance between the two plates of the sensor. FDC2214 is a capacitive digital converter in a compact package, which combines a resonant circuit driver, a signal processer, a 28-bit analog-to-digital converter, and an Inter-Integrated Circuit (I2C) interface. Moreover, considering that the measurement circuit is far away from the controller, each measurement circuit board uses a voltage regulator. The size of the measurement circuit board is 23 mm × 9 mm, which can be installed entirely inside the cavity of the distal phalanx, as shown in Figure 2.

To facilitate the connection with the prosthesis controller, a slave microcontroller (STM32F401CEU6, STMicroelectronics, Geneva, Switzerland) was used to control five sensor measurement modules and communicate with the prosthetic hand controller. An I^2C bus was used to connect five sensor modules. To reduce the number of cables, time-division multiplexing was adopted to control five measurement circuits. All sensor modules' serial data lines (SDA) were directly connected to the host (slave MCU). While five serial clock lines (CLK) were connected to the channel out of a multiplexer (CD4051, Texas Instruments, Texas, USA), the CLK of the host was connected to the common terminal COM of the multiplexer, as shown in Figure 3. The sensor controller controls the multiplexer timing sequence to ensure that only one slave CLK is connected to the host at each moment. In this case, only the module connected to the host could communicate effectively, and others kept running in the background. The sensor controller operates each sensor module in sequence at an interval of 2 ms. The capacitance measurement period was set to 9.2 ms. Considering the data transmission time (approximately 0.5 ms), we set the measurement frequency of each sensor module to 100 Hz. The sensor controller polled all five sensors in a round-robin fashion, and it took 10 ms to complete a measurement cycle (five sensors). After completing a cycle, the host sent all measurement data to the prosthesis controller.

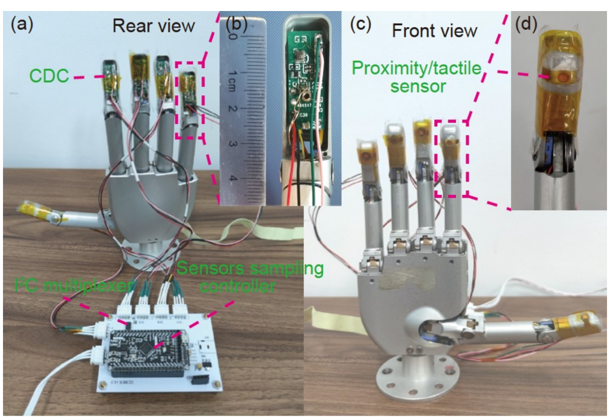

Figure 2 (Color online) Rear view (a) and front view (c) photographs of the prosthetic hand with the proximity-tactile sensor system. Close-up view of the sensor sampling circuit board installed in the fingertip (b) and proximity-tactile sensor attached to the fingertip surface (d).

2.3 Calibration of PTS

The proposed flexible PTS was attached to the fingertip of the HIT V hand prosthesis and fixed by PI tapes. The flexible base of the sensor conforms to the fingertip. Because the fingertip's surface has a specific curvature, the electrodes and dielectric layer of the sensor may bend, which may change the output characteristics of the sensor. In addition, the prosthetic hand is mainly made of aluminum alloy, and its electrostatic induction will affect the capacitance measurement of the sensor. Furthermore, we should consider the influence of electromagnetic noise from the motor. Traditionally, the calibration setup is pure and offline, in which the sensor is placed on an insulated plate, independent of the robot's operation. To get realistic characteristics, we calibrated the PTS on the fingertip in the working state.

The setup of the proximity calibration is shown in Figure 4(a). A machine vise fixes a finger with the proposed

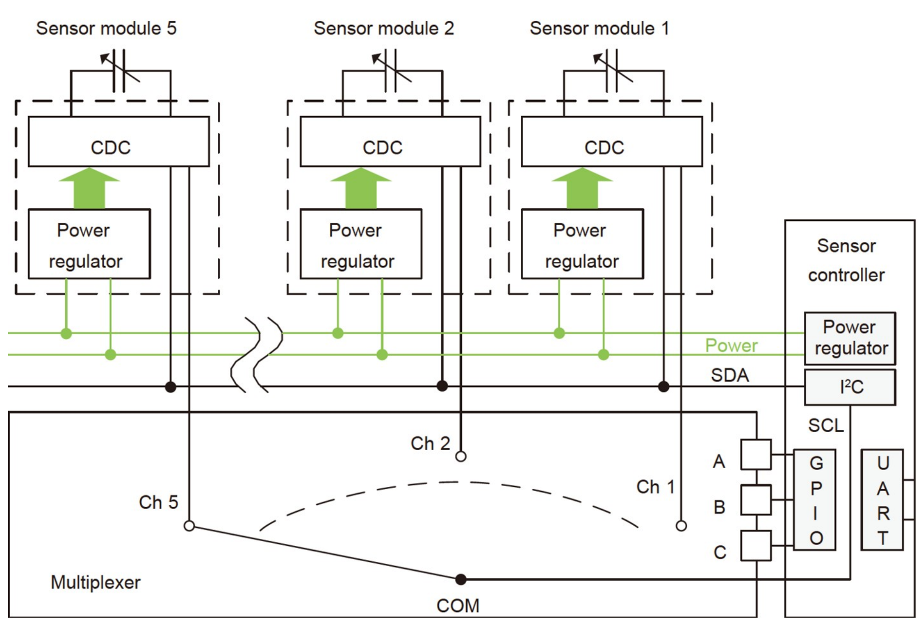

Figure 3 (Color online) Connection method of the five sensor modules for a hand and the measurement system.

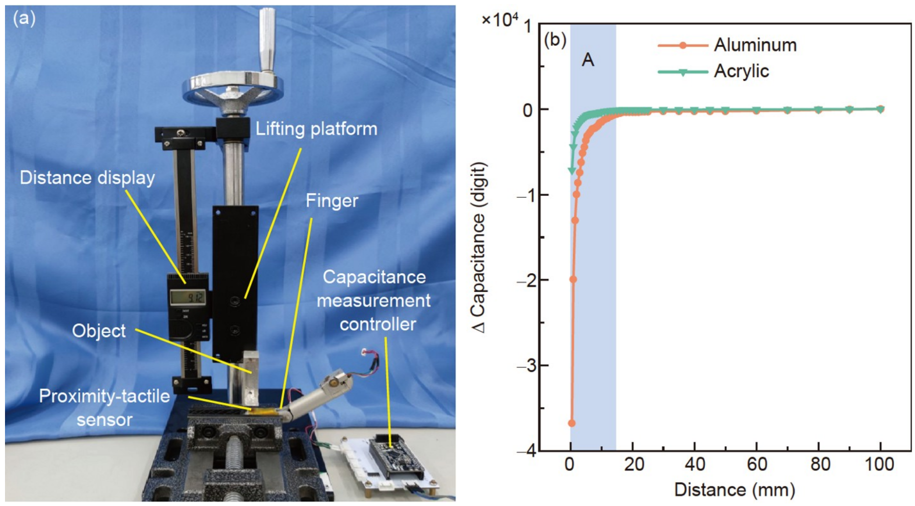

Figure 4 (Color online) Proximity sensing performance. (a) Experimental setup. (b) Calibration results for the sensor working as the proximity sensor and one with aluminum for conductive and dielectric objects approaching the sensor.

sensor and measurement circuit under the lifting platform. The lifting platform was installed with the test object (aluminum alloy and acrylic). The distance between the object and sensor was manually adjusted, and the measurement system's output was recorded. The variations in the sensor output and distance during the calibration are shown in Figure 4(b). The results show that the sensor output changes with the distance. Particularly, within the 15 mm distance (range A in Figure 4(b)), the output of the sensor drastically decreases as the distance decreases, and the closer the distance, the greater the change rate. Hence, proximity sensing has high sensitivity in short distances. Moreover, the response curves of objects of various materials are different. The output amplitude of non-metallic acrylic sensors is much smaller than that of metal materials, but the trend is similar. Therefore, although the proximity detection distance of an object depends on the object's electrical characteristics, the approach of the object can still be detected within a certain range (range A in Figure 4(b)).

The tactile calibration setup is shown in Figure 5(a). A machine vise fixed a finger with a flexible sensor and measurement circuit. The measurement system and finger motor were connected with the prosthesis controller. The fingertip pressed the probe mounted on a six-dimensional force sensor (Nano17, ATI Industrial Automation, Apex, NC, USA), and Nano17 measures the actual contact force. The driving voltage of the finger motor was gradually increased, and the outputs of Nano17 and the PTS were recorded. The calibration data and curve fitting are shown in Figure 5(b). The relationship between the sensor output and contact force was determined by the linear least squares as follows:

$$C_{out} = 5208.01 \cdot F + 13172.83, \quad (1)$$

where C_{out} is the output value of the sensor, F is the contact force; and the R-square is 0.99682.

2.4 Contact detector

The PTS could measure the distance and contact force of the

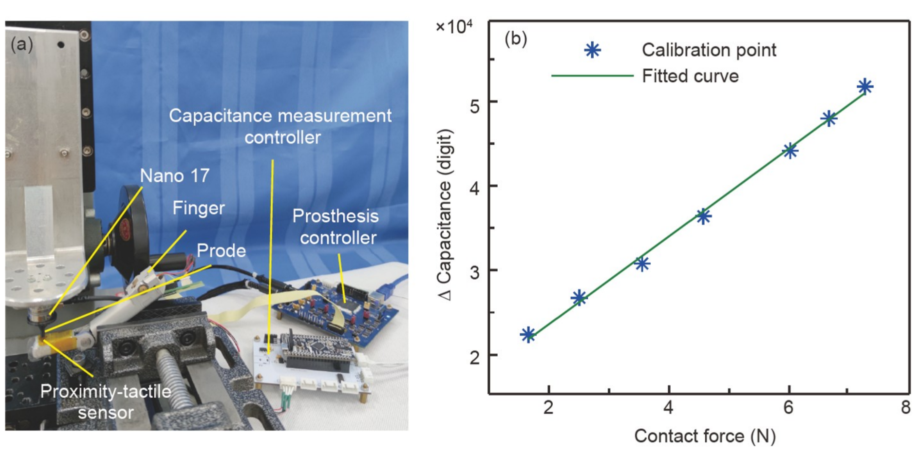

Figure 5 (Color online) Tactile sensing performance. (a) Experimental setup. (b) Calibration results for the sensor working as the tactile sensor.

object before and after contact, respectively. The sensor outputs of the two phases are both the capacitance value, whereas the output characteristics of the two phases are different. The output capacitance of the sensor decreases as the distance of the object decreases before contact, whereas it increases as the contact force increases after contact. Therefore, during a complete approach-touch-grasping process, an inflection point will appear on the curve of the sensor output versus time near the contact. At the same time, the sensor output signal will undergo local oscillation under the influence of mechanical vibration when the contact is made. Previous research passed raw tactile signals through a high-pass filter to detect contact events, which appear as extrema in the high-pass signal [36].

We employed a discrete-time Butterworth high-pass filter with a cut-off frequency of 5 Hz for a 100 Hz measuring rate of the sensor. As shown in Figure 6, before the grasping, values ranging above the specific threshold were considered contact detection. The gradual decrease in the raw signal refers to an approaching object. Eventually, the object was contacted, denoted by a peak in the high-pass signal. Therefore, when the amplitude of the high-pass signal exceeds the pre-set threshold, indicating a contact occurs, the output of the sensor switches to the tactile sensing mode.

3 Control and experiments

We employed the proposed sensor and HIT V prosthetic hand to perform experiments to verify the usefulness of the proposed sensor in prosthesis grasping and human-machine neural interface. The study protocol involving humans was approved by the local ethics committee of the Harbin Institute of Technology (HIT-2021009).

The proposed PTS enables object distance and contact force sensing successively before and after grasping. Before grasping, we controlled each finger motion based on the distance of the object independently rather than along the pre-set trajectory to approach the object. For the multi-fingered hand, all fingers performed this control to form a pre-grasping gesture fitting the object shape eventually before contact. Then, all fingers simultaneously flexed to grasp the object; because of the matched gesture, all fingers touched the object simultaneously to achieve a stable grasp. After contact, the sensor turned to the contact force sensing, and the hand performed the grasping force closed-loop control based on tactile.

3.1 Pre-grasping control based on proximity information

In this section, we describe a pre-grasping control method based on the proximity sensing of the proposed sensor. In this method, the pre-grasping process is broken down into individual, independent controls according to the distance between the fingertip and grasped object surface for each finger. The movement of each finger was controlled to stop at the same distance from the object's surface before contact. As shown in Figure 7, the finger control was similar to the damping control typically utilized in force control. In this method, the joint speed of the finger was controlled based on the distance between the fingertip and object proportionally. The closer the distance, the slower the finger speed. The finger stopped moving when it reached the desired distance. The joint speed was determined by

$$\dot{\theta}_{\text{ref-F}} = K_1(d_{\text{F}} - d_{\text{ref}}), \quad (2)$$

so the reference value of the finger position controller was determined by

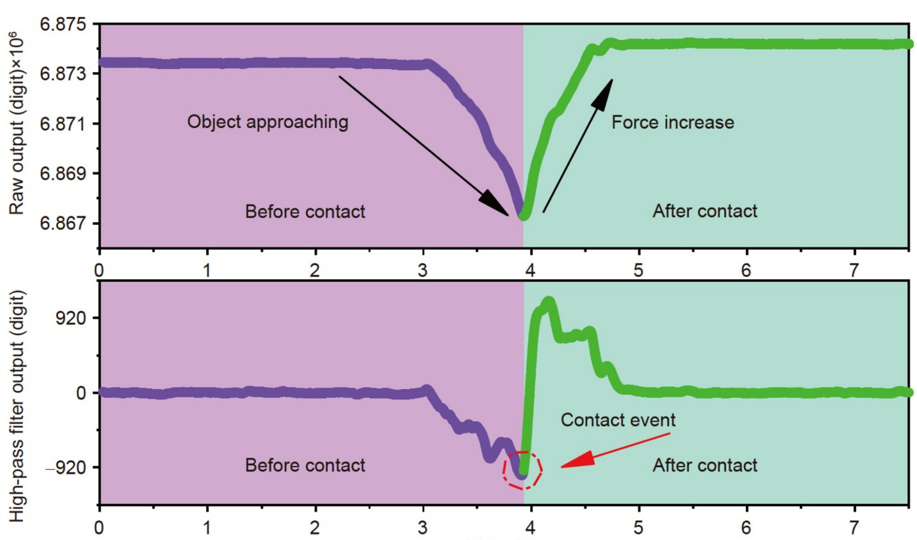

Figure 6 (Color online) Sensor raw output and its result through a high-pass filter to detect the contact event.

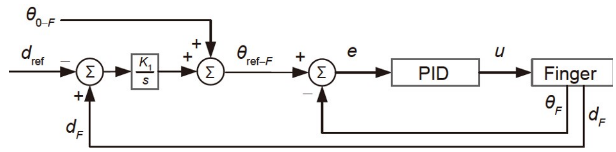

Figure 7 Schematic of the proximity-based pre-grasping control.

$$\theta_{\text{ref-F}} = \theta_{0-\text{F}} + K_1 \int (d_{\text{F}} - d_{\text{ref}}) \mathrm{d}t, \tag{3}$$

where $\theta_{\text{ref-F}}$ is the target value in the angle-based PID control, $\theta_{0\text{-F}}$ is the joint angle at the initiation of feedback control, and K_1 is the feedback gain. We adjust K_1 to an appropriate value experimentally. d_{F} is the distance value measured by the proposed sensor, and d_{ref} is the value sought for the distance.

After all fingers stopped near the object surface and formed a pre-grasping gesture adjusting to the object's shape, all fingers simultaneously flexed to grasp the object.

In the verification experiment, the grasped object was an aluminum alloy object composed of two cylinders with different diameters. The experimental results are shown in Figure 8. Due to manufacturing errors, the output characteristics of each sensor are different. Different desired values were set according to the calibration. First, all fingers flexed at the same speed. While the thumb and little finger were close to the object's surface, they reached the set desired position at first. Then, the motors turned off; the index finger, ring finger, and middle finger reached the set position in turn; and a pre-grasping gesture was formed. Lastly, the five fingers simultaneously flexed to grasp the object.

3.2 Grasping force control based on tactile information

Based on the previous tactile calibration results, we conducted a step force tracking experiment on the grasping force. The PTS on the fingertip measured the contact force, and the prosthesis controller controlled the finger to track the expected force trajectory according to the measurement result. The expected force was increased stepwise from 2.0 N to 2.5, 3.0, and 3.2 N; then reduced to 3.0, 2.5, and 2.0 N; and maintained at each level for 5 s. We employed the classic PID controller. The parameters were adjusted to get better control results. Due to the measurement frequency of the PTS measurement system, the closed-loop control frequency of the force was limited to 100 Hz in the experiment. The results are shown in Figure 9, in which the maximum force error is 0.4 N and the steady-state force error is 0.03.

3.3 Human-machine interaction control

To evaluate the effectiveness of the proposed sensor for EMG prosthetic hand applications, we conducted a human-machine neural interaction experiment. The scheme of the control is shown in Figure 10. Different from the automatic control mentioned above, in this experiment, the EMG signal was used to control the HIT V hand in real time. Moreover, unlike direct EMG control, the fingers first flexed based on proximity to form a pre-grasping gesture rather than along the fixed trajectory. That is, EMG was the high-level motion instruction, and the low-level control was based on proximity. After the pre-grasping gesture, the subject drove all fingers to contact the object. Then, the grasping force measured by the PTS was transmitted to the subject through the transcutaneous electrical nerve stimulation (TENS). Accordingly, the subject adjusted the force to track the expected force.

The experimental environment is shown in Figure 11(a). To simplify the control, only the thumb and index finger were involved in grasping, and the two fingertips were

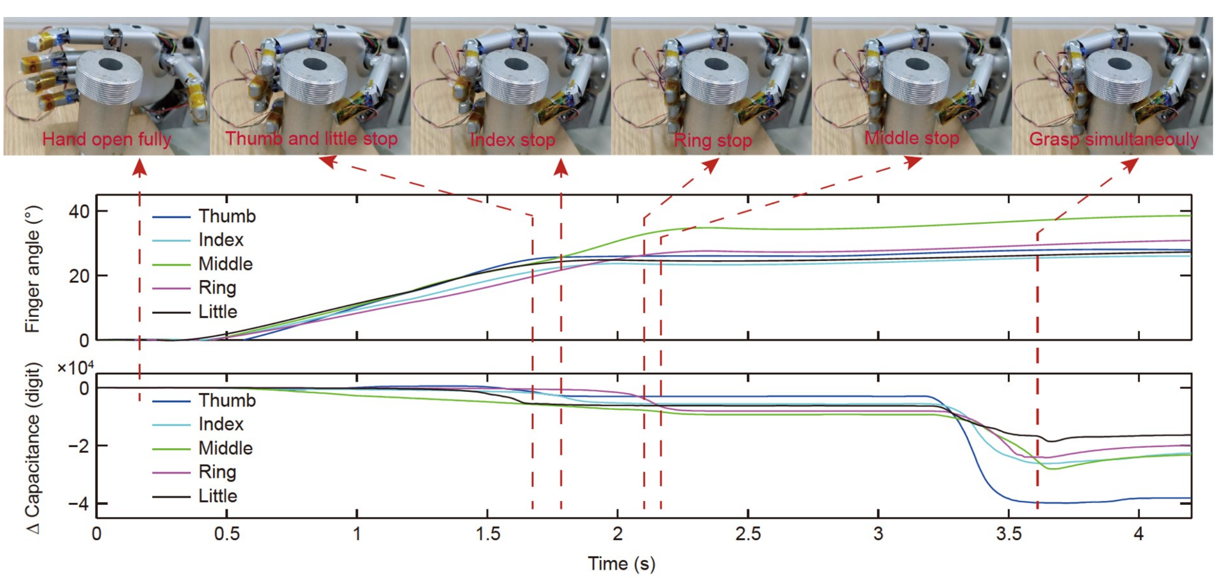

Figure 8 (Color online) Sequence of pre-grasping based on proximity for the HIT V hand.

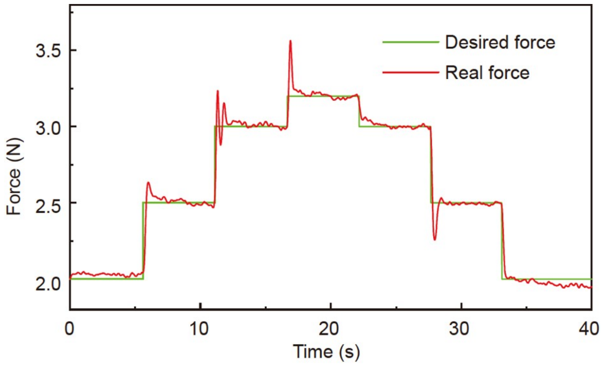

Figure 9 (Color online) Performance of the contact force tracking task.

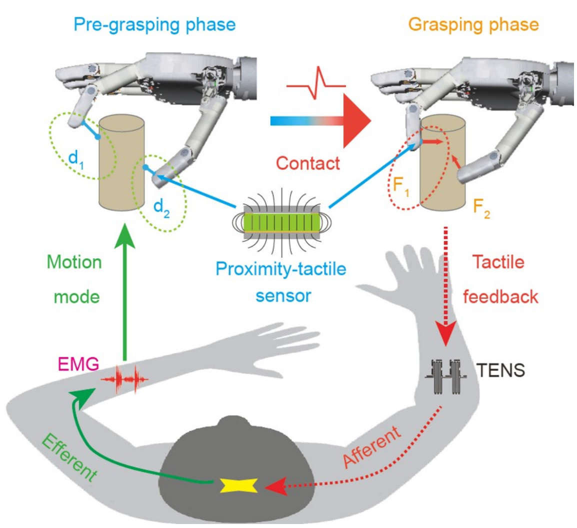

Figure 10 (Color online) Scheme of the human-machine interaction control based on the proximity-tactile sensor.

equipped with the PTSs. Two EMG electrodes (13E200, Otto Bock Healthcare GmbH, AT) were placed on the wrist flexor and extensor muscles of the forearm of the subject. The EMG electrode outputted the root mean square of the raw EMG signal. The higher the muscle contraction strength, the higher the amplitude of the electrode output signal. The signals of the two EMG electrodes were classified into three types: flexion, extension, and relaxation. Before touching the object, the three EMG types correspond to three motion modes of the prosthetic hand: closing, opening, and stopping. Two round gel electrodes were placed on the contralateral forearm to deliver the TENS signal. The grasped object was a hollow iron round can. To measure the posture of the iron can, an IMU module was fixed on the iron can to record the posture angles in the form of Euler angle and acceleration of the object during the experiment. The measurement frequency was 100 Hz.

The control process is shown in Figure 11(b). The experiment started, the subject contracted the flexor muscles to trigger the finger flexion, and the PTSs measured the distances of the object. At the same time, the fingers were controlled based on proximity. During this process, the fingers would not outspread unless the extensor was active. After the index finger and thumb formed the pre-grasping gesture, the TENS delivered a pulse to indicate to the subject that the gesture had been completed. Then, the subject relaxed the muscles and contracted the flexor again, controlling the two fingers to simultaneously grasp the object. Afterward, the subject controlled the grasping force via flexor contraction. The value of the grasping force was proportionally determined by the EMG output amplitude of the flexor muscle. The PTS measured the actual contact force of the index finger. The electrical stimulation electrode delivered the TENS pulse signal to the subject, of which the pulse magnitude was proportional to the actual grasping force. The TENS induced the sensation on the skin. The greater the grasping force, the higher the magnitude of the stimulation pulse, and the stronger the sensation on the skin. The subject perceived the intensity of the sensation, estimated the actual grasping force accordingly, and adjusted the grasping force to track the reference force. In this experi-

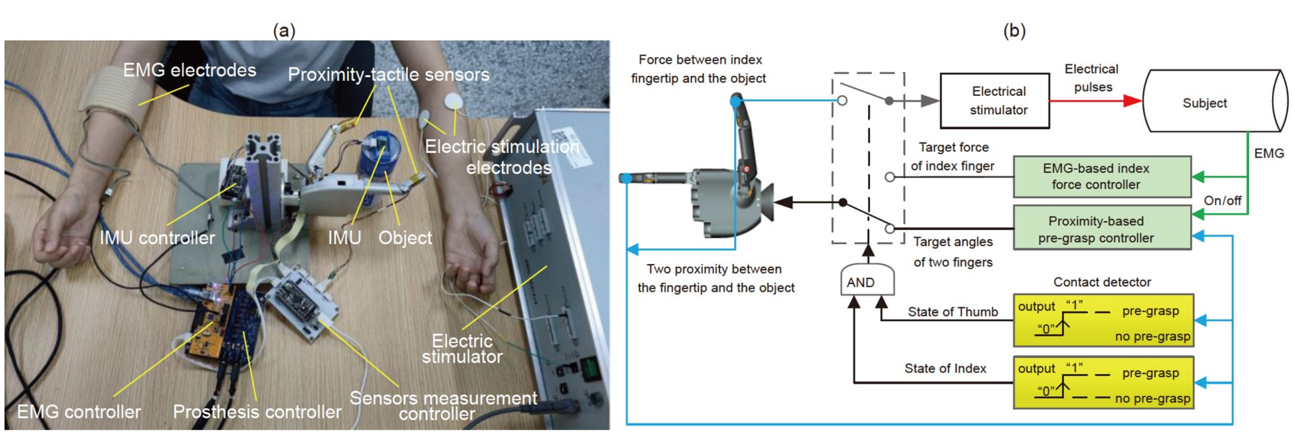

Figure 11 (Color online) (a) Experimental setup of the closed-loop EMG control with the proximity-tactile sensors through a neural interface. (b) Control modules for the closed-loop EMG control with the pre-grasping through a neural interface.

ment, the reference grasping force trajectory was a trapezoidal curve, gradually increasing from 2.0 N to 5.8 N within 5 s, maintaining 5 s after reaching 5.8 N, and gradually decreasing to 2.0 N within 5 s. Taking into account human recognition ability, the period of the TENS feedback was 100 ms, the pulse width of the stimulation pulses was 10 ms, and the magnitude was adjusted in the range of 0–20 V.

In addition, to verify the effectiveness of pre-grasping based on proximity, a set of comparative experiments was conducted, in which the experimental configure remained; only proximity was not involved in the control. Fingers were completely controlled by EMG signals, and the thumb and index finger moved along the constant trajectories simultaneously.

As shown in Figure 12(a), the two fingers simultaneously flexed toward the grasped object with the participation of proximity. Because the thumb fingertip was initially closer to the object than the index, the thumb reached the desired position first while the index finger kept moving. When the index fingertip reached the desired distance from the object, the prosthetic hand formed a pre-grasping gesture around the object in which all fingertips stopped near the object's surface. Then, the subject controlled all fingers to flex toward the object simultaneously to grasp the object. For the pre-grasping gesture, the thumb and index fingertips were almost the same distance from the object surface, and all fingers touched almost at the same time. No significant posture and position change occurred in the object. While the slight posture change may be due to the asymmetric grasp configuration of two fingertips around the object, due to the anthropomorphic configuration of the HIT V hand, the thumb and index finger were not strictly opposed. The object automatically adjusted its posture in the final balance under the two asymmetric contact forces.

In the absence of proximity, the experimental results are shown in Figure 12(b). Two finger motors synchronously turned on/off triggered by the EMG. While the thumb was closer, the object was first touched and then moved forward. Due to the light mass, the object moved and slightly tilted toward the index finger under the push of the thumb. After approximately 0.5 s, the index finger touched the object. Because the object's posture had been tilted instead of upright, the contact forces of two fingers cannot form a perfect two-force balance. Therefore, under the force of the index finger, the object greatly deflected until a new balance. Compared with the initial posture, the object deflected by 8.34°. In addition, due to the tilted posture of the object, the contact between the fingertip and object was not normal, especially the thumb friction with the ground and the force of the index finger. The thumb fingertip slid on the object's surface. This shearing motion damaged the contact between the sensor and the object, which resulted in a drastic change in the output of the sensor, and might even damage the flexible sensor and fail to measure force.

To verify the universality of the method, we compared the performance on multiple positions in two conditions using the proposed method and not using it. Two conditions were defined as the control group (Control group) and reference group (Ref group). Each group included ten positions in the grasping space of the prosthetic hand. The variation of the three Euler angles (row, pitch, and yaw) of the grasped object during the grasping is shown in Figure 13 in the form of boxplots. A *t*-test statistically analyzed the results. The result showed that the posture changes were significantly decreased in the control group compared to the reference group ($P < 0.001$).

The results of the closed-loop control of grasping force based on the human-machine neural interface are shown in

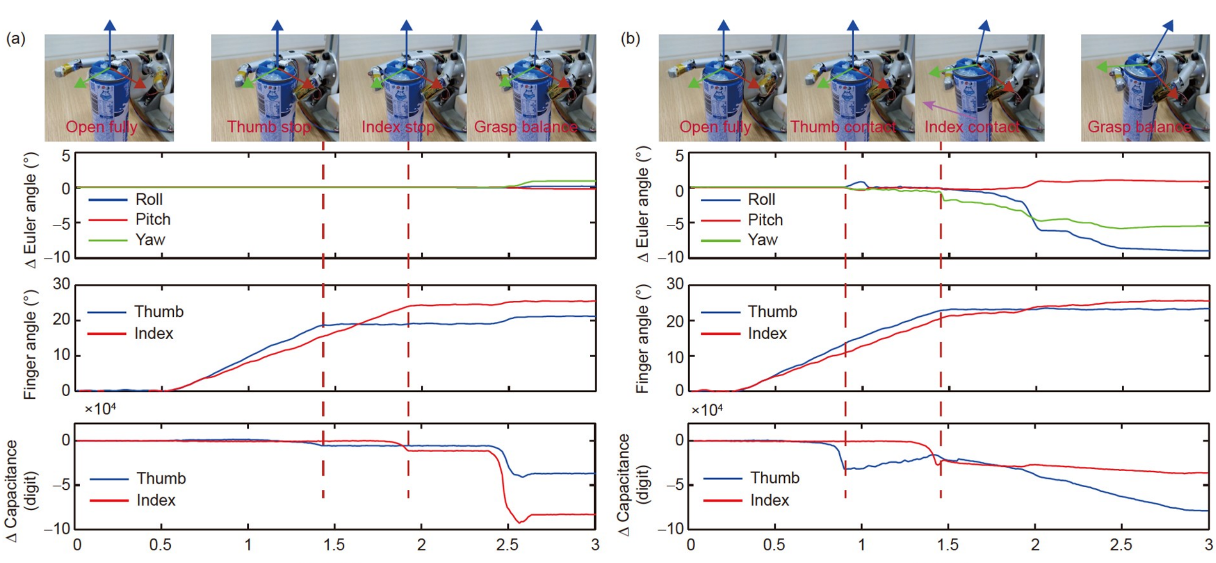

Figure 12 (Color online) Process of EMG grasping. (a) Grasping process with proximity. (b) Grasping process without proximity.

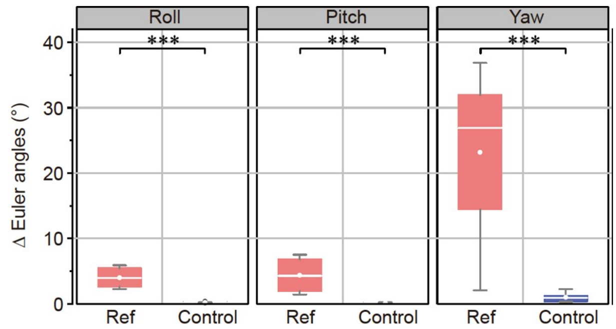

Figure 13 (Color online) Summary results of the variation of Euler angles of the grasped object for the grasping using the pre-grasping based on proximity (Control group) and not using it (Ref group). Horizontal bars indicate the statistically significant differences (***, $P < 0.001$).

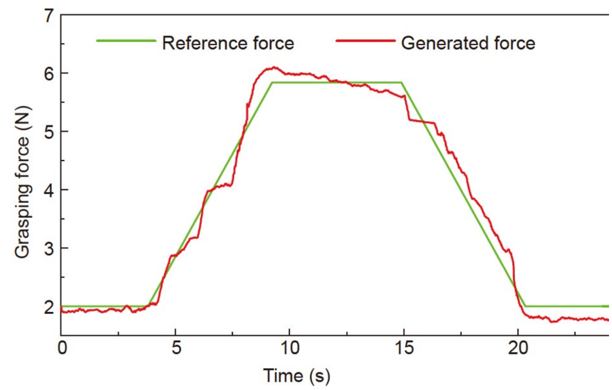

Figure 14 (Color online) Grasping force trajectory for the EMG control force tracking task based on the neural interface.

Figure 14. During the whole process, the overall average force error was 0.18 N, and the maximum error force was 0.53 N. The grasping force generated by the subject was generally consistent with the reference force, which indicated that the subject could estimate the grasping force based on electrical stimulation. Errors were found between the generated and expected forces. These errors occurred because the resolution of the subject's estimated real grasping force, which relied on the TENS coding, was not as precise as that of the physical sensor, only roughly several discrete levels. Inevitably, there were errors between the actual and estimated values. In addition, the grasping force of the prosthetic hand was determined by the flexor contraction, and it was difficult to keep the strength of muscle contraction constant for a long time. Because long-term muscle contraction would also cause fatigue, it may cause the EMG signal intensity to decrease over time. Therefore, due to the nature of the sensory perception of the human in combination with the variability of the myoelectric control signals, the generated grasping force was not stable enough. Moreover, the limitation of the force controller in part caused vibration and error in the generated force.

4 Conclusions

This paper proposes a control method based on a new type of flexible PTS to improve the grasping performance of prosthetic hands. Initially, it introduces the sensing principles and structure of the sensor. We designed an integrated measurement system to improve measurement accuracy and reliability. Moreover, a pre-grasping formation method is proposed based on proximity sensing. An appropriate pre-grasping gesture can be formed according to the object's shape before touching, which has been verified with an irregularly shaped object. The expected force tracking experiment based on the tactile sensing of the sensor was also performed to verify the accurate force control. Finally, proximity-based pre-grasping was introduced in the closed-loop control of the prosthetic hand based on the human-machine neural interface. The experimental results prove that the pre-grasping method could effectively improve the grasping stability. Hence, there is a promising potential in restoring sensory feedback function for amputees using the PTS.

Future work will focus on recognizing object properties based on the sensor output capacitance. In addition, advanced robot control algorithms based on proximity will be employed to improve grasping compliance. Proximity and tactile sensing can also be used to provide amputees with spatial and grasping information through sensory feedback to improve users' perception and grasping ability.

This work was supported by the National Key R&D Program of China (Grant No. 2018YFB1307201) and the National Natural Science Foundation of China (Grant Nos. U1813209 and 51875120).

1 Belter J T, Segil J L, Dollar A M, et al. Mechanical design and performance specifications of anthropomorphic prosthetic hands: A review. J Rehabil Res Dev, 2013, 50: 599–617
2 Kasim M A A, Low C Y, Ayub M A, et al. User-friendly LabVIEW GUI for prosthetic hand control using Emotiv EEG headset. Procedia Comput Sci, 2017, 105: 276–281
3 Setiawan J D, Ariyanto M, Munadi M, et al. Grasp posture control of wearable extra robotic fingers with flex sensors based on neural network. Electronics, 2020, 9: 905
4 Geethanjali P. Myoelectric control of prosthetic hands: State-of-the-art review. Med Devices-Evid Res, 2016, Volume 9: 247–255
5 Dalley S A, Varol H A, Goldfarb M. A method for the control of multigrasp myoelectric prosthetic hands. IEEE Trans Neural Syst Rehabil Eng, 2012, 20: 58–67
6 Yang B, Jiang L, Hu J, et al. A compact control system and a myoelectric control method for multi-DOFs prosthetic hand. In: IEEE International Conference on Real-time Computing and Robotics. Irkutsk, 2019. 592–597
7 Kuiken T A, Miller L A, Turner K, et al. A comparison of pattern recognition control and direct control of a multiple degree-of-freedom transradial prosthesis. IEEE J Transl Eng Health Med, 2016, 4: 1–8
8 Hahne J M, Biessmann F, Jiang N, et al. Linear and nonlinear re-

gression techniques for simultaneous and proportional myoelectric control. IEEE Trans Neural Syst Rehabil Eng, 2014, 22: 269–279

9 Yang D, Zhao J, Gu Y, et al. EMG pattern recognition and grasping force estimation: Improvement to the myocontrol of multi-DOF prosthetic hands. In: IEEE/RSJ International Conference on Intelligent Robots and Systems. St. Louis, 2009. 516–521

10 Yang W, Yang D, Liu Y, et al. Decoding simultaneous multi-DOF wrist movements from raw EMG signals using a convolutional neural network. IEEE Trans Hum-Mach Syst, 2019, 49: 411–420

11 Koyama K, Suzuki Y, Ming A, et al. Integrated control of a multi-fingered hand and arm using proximity sensors on the fingertips. In: IEEE International Conference on Robotics and Automation. Stockholm, 2016. 4282–4288

12 de Maria G, Falco P, Natale C, et al. Integrated force/tactile sensing: The enabling technology for slipping detection and avoidance. In: IEEE International Conference on Robotics and Automation. Seattle, 2015. 3883–3889

13 Geravand M, Flacco F, de Luca A. Human-robot physical interaction and collaboration using an industrial robot with a closed control architecture. In: IEEE International Conference on Robotics and Automation. Karlsruhe, 2013. 4000–4007

14 Borisov I I, Borisova O V, Krivosheev S V, et al. Prototyping of EMG-controlled prosthetic hand with sensory system. IFAC-PapersOnLine, 2017, 50: 16027–16031

15 Gentile C, Cordella F, Rodrigues C R, et al. Touch-and-slippage detection algorithm for prosthetic hands. Mechatronics, 2020, 70: 102402

16 Shi C, Yang D, Zhao J, et al. Computer vision-based grasp pattern recognition with application to myoelectric control of dexterous hand prosthesis. IEEE Trans Neural Syst Rehabil Eng, 2020, 28: 2090–2099

17 Hsiao K, Nangeroni P, Huber M, et al. Reactive grasping using optical proximity sensors. In: IEEE International Conference on Robotics and Automation. Kobe, 2009. 2098–2105

18 Chiurazzi M, Garozzo G G, Dario P, et al. Novel capacitive-based sensor technology for augmented proximity detection. IEEE Sens J, 2020, 20: 6624–6633

19 Castellanos-Ramos J, Trujillo-Leon A, Navas-Gonzalez R, et al. Adding proximity sensing capability to tactile array based on off-the-shelf FSR and PSoC. IEEE Trans Instrum Meas, 2020, 69: 4238–4250

20 Novak J L, Feddema J T. A capacitance-based proximity sensor for whole arm obstacle avoidance. In: IEEE International Conference on Robotics and Automation. Nice, 1992. 1307–1314

21 Navarro S E, Schonert M, Hein B, et al. 6D proximity servoing for preshaping and haptic exploration using capacitive tactile proximity sensors. In: IEEE/RSJ International Conference on Intelligent Robots and Systems. Chicago, 2014. 7–14

22 Hirai Y, Suzuki Y, Tsuji T, et al. High-speed and intelligent pre-grasp motion by a robotic hand equipped with hierarchical proximity sensors. In: IEEE/RSJ International Conference on Intelligent Robots and Systems. Madrid, 2018. 7424–7431

23 Hasegawa S, Yamaguchi N, Okada K, et al. Online acquisition of close-range proximity sensor models for precise object grasping and verification. IEEE Robot Autom Lett, 2020, 5: 5993–6000

24 Tavakoli M, Lopes P, Lourenco J, et al. Autonomous selection of closing posture of a robotic hand through embodied soft matter capacitive sensors. IEEE Sens J, 2017, 17: 5669–5677

25 Yousef H, Boukallel M, Althoefer K. Tactile sensing for dexterous in-hand manipulation in robotics—A review. Sens Actuat A-Phys, 2011, 167: 171–187

26 Johansson R S, Flanagan J R. Coding and use of tactile signals from the fingertips in object manipulation tasks. Nat Rev Neurosci, 2009, 10: 345–359

27 Peerdeman B, Boere D, Witteveen H, et al. Myoelectric forearm prostheses: State of the art from a user-centered perspective. J Rehabil Res Dev, 2011, 48: 719–737

28 Biddiss E, Beaton D, Chau T. Consumer design priorities for upper limb prosthetics. Disabil Rehabil-Assist Technol, 2007, 2: 346–357

29 Stephens-Fripp B, Alici G, Mutlu R. A review of non-invasive sensory feedback methods for transradial prosthetic hands. IEEE Access, 2018, 6: 6878–6899

30 Ciancio A L, Cordella F, Barone R, et al. Control of prosthetic hands via the peripheral nervous system. Front Neurosci, 2016, 10: 116

31 Konstantinova J, Stilli A, Althoefer K. Force and proximity fingertip sensor to enhance grasping perception. In: IEEE/RSJ International Conference on Intelligent Robots and Systems. Hamburg, 2015. 2118–2123

32 Segil J, Patel R, Klingner J, et al. Multi-modal prosthetic fingertip sensor with proximity, contact, and force localization capabilities. Adv Mech Eng, 2019, doi: 10.1177/1687814019844643

33 Lee H K, Chang S I, Yoon E. Dual-mode capacitive proximity sensor for robot application: Implementation of tactile and proximity sensing capability on a single polymer platform using shared electrodes. IEEE Sens J, 2009, 9: 1748–1755

34 Tsuji S, Kohama T. Self-capacitance proximity and tactile skin sensor with shock-absorbing structure for a collaborative robot. IEEE Sens J, 2020, 20: 15075–15084

35 Zeng B, Fan S, Jiang L, et al. Design and experiment of a modular multisensory hand for prosthetic applications. Industrial Robot, 2017, 44: 104–113

36 Patel R, Cox R, Correll N. Integrated proximity, contact and force sensing using elastomer-embedded commodity proximity sensors. Auton Robot, 2018, 42: 1443–1458